28 Dec 1990

Uniform Stationary-phase Methods For Energy Spectra Resulting From Collisions In A Complex Potential: Penning And Associative Ionization Of He*(2³S)+He*(23S)

Ronald James Bieniek
Missouri University of Science and Technology, bieniek@mst.edu

M. W. Muller

M. Movre

Recommended Citation

R. J. Bieniek et al., "Uniform Stationary-phase Methods For Energy Spectra Resulting From Collisions In A Complex Potential: Penning And Associative Ionization Of He*(2³S)+He*(23S)," *Journal of Physics B: Atomic, Molecular and Optical Physics*, vol. 23, no. 24, pp. 4521 - 4538, IOP Publishing, Dec 1990.
The definitive version is available at https://doi.org/10.1088/0953-4075/23/24/011

Uniform stationary-phase methods for energy spectra resulting from collisions in a complex potential: Penning and associative ionization of $He^*(2^3S)+He^*(2^3S)$

J. Phys. B: At. Mol. Opt. Phys. **23** (1990) 4521–4538. Printed in the UK

Uniform stationary-phase methods for energy spectra resulting from collisions in a complex potential: Penning and associative ionization of $He^*(2^3S)+He^*(2^3S)$

R J Bieniek†, M W Müller‡ and M Movre§

† Physics Department and Laboratory for Atomic and Molecular Research, University of Missouri-Rolla, Rolla, MO 65401, USA
‡ Fachbereich Physik, Universität Kaiserslautern, D-6750 Kaiserslautern, FRG
§ Institute of Physics of the University 41000 Zagreb, Yugoslavia

Received 27 July 1990, in final form 24 September 1990

Abstract. Heavy-particle collisions involving strong electronic coupling can be conveniently described by using a complex (optical) potential in the entrance channel. Uniform JWKB stationary-phase techniques are used to evaluate T-matrix elements for transitions where an electron is ejected. The semi-analytic expressions for the resulting electron energy spectra are no more difficult to implement than corresponding ones for totally real potentials. Numerical results are reported for Penning and associative ionization from subthermal $He^*(2^3S)+He^*(2^3S)$ collisions. These are in excellent agreement with fully quantal, complex-potential computations. The stationary-phase expressions for T-matrix elements and differential cross sections are employed to elucidate the rapid and slow rainbow interference oscillations in the spectra, including the significant effects of turning points and the imaginary width of the entrance-channel potential.

1. Introduction

When a metastable atom collides with a target, a perturbation is induced in the electronic configuration that allows a transitional path through autoionization of the quasimolecule. Basically, a target electron can jump to the metastable's ground state, while the metastable's excited electron is ejected (Hotop and Niehaus 1970, Bell 1970). Penning ionization (PI) results if the former metastable atom is asymptotically free, and associative ionization (AI) if it is bound in a molecular ion. As part of a recent comprehensive review of these and related processes, Niehaus (1990) traces the historical development of models and theories of PI and AI over the last two decades. Nakamura (1968a, 1968b, 1969) and Mori (1969) employed Fano's (1961) theory of the interaction of a discrete state with a continuum in which it is embedded to derive an early quantal formalism for wavefunctions and matrix elements. In a semiclassical view, the energy of the ejected electron equals the potential difference at the point of transition. The variation of the potential difference with internuclear separation was utilized to explain total cross sections and general shape of electron energy spectra in pioneering experimental studies (Schmeltekopf and Gilman 1967, Cermak and Herman 1968, Hotop and Niehaus 1968, 1969, 1970). By applying simple JWKB techniques to the overlap integral of the heavy-particle wavefunctions, the main interference phenomena underlying the electron spectra were revealed (Miller 1970, Gerber and Niehaus 1976). Some of the most significant of these are Airy-type rainbow interference

0953-4075/90/244521+18$03.50

structures that arise from transitions at two different internuclear separations (Morgner and Niehaus 1979). This phenomenon arises in many other processes, including far-wing and half-collisional photon processes (Bieniek and Streeter 1983, and references therein).

A variety of semiclassical and JWKB stationary-phase methods have been used to describe such type of spectra (Miller 1970, Szudy and Baylis 1975, Gerber and Niehaus 1976, Bieniek and Streeter 1983, Tellinghuisen 1985). Sayer *et al* (1980) experimentally observed the slow Airy-envelope undulations in the collisionally induced far-wing of a cesium forbidden line, broadened by rare gas perturbers. Although this is, essentially, the spectral equivalent of PI/AI, the Airy rainbow undulations have been much harder to observe in PI/AI because of the generally lower resolution of experimental electron spectroscopy methods (Morgner and Niehaus 1979, Müller *et al* 1987, Merz *et al* 1989, 1990).

However, in both spectral line broadening and collisionally induced ionization, more rapid oscillations in the spectra, arising from interference between initial and final wavefunctional phases, have been washed out in experiments because of phase averaging from the large number of collisional angular momenta involved (Szudy and Baylis 1975, Bieniek 1977). These rapid oscillations are observed, though, under an Airy-type envelope, in half-collision photodissociation and fluorescent dissociation of diatomics, because only one angular momenta is basically involved (Eisel *et al* 1979, Tellinghuisen *et al* 1980, Gadea *et al* 1983, Noll and Schmoranzer 1987, Master *et al* 1990). Stationary-phase methods of analytically evaluating T-matrix elements have proved to be an accurate and insightful means of explaining both the rapid and slow oscillations in the resulting continuum spectra (Tellinghuisen 1985, Schmoranzer *et al* 1990). However, with the advances in experimental mixed-beam technology (Müller *et al* 1987), subthermal collisional energies for PI/AI are now obtainable in which only a few angular momenta contribute. There is hope then that rapid-oscillation phenomena may become unambiguously observable in PI/AI electron energy spectra.

The stationary-phase (and even the quantal) techniques that have been used to explain far-wing line spectra have neglected the effect of the transitions on the entrance channel. Although a distorted-wave approach is almost always accurate in such cases because spectral coupling is weak compared to intermolecular potentials, the same is not the case for PI/AI where cross sections are much larger. The entrance channel can be significantly perturbed by the strong transitional coupling. Since there is an infinite set of final free states to consider, their total effect can be most easily (and insightfully) described by the addition of an imaginary width to the potential of heavy-particle motion in the entrance channel (O'Malley 1967, Miller 1970, Bieniek 1978, Berman *et al* 1983, Saha *et al* 1983, Jones and Dahler 1988; see Weiner *et al* 1990 for a review of an alternative approach to AI). If the final states effectively form a complete set, as is generally the case in PI/AI because of the large electronic energy range, then the complex potential is local (Bieniek 1980b, Lam and George 1984, Mündel and Domcke 1984, Morgner 1990).

If the transitional coupling is small, then the imaginary part of the potential can be neglected in the production of the initial heavy-particle wavefunction, even though the imaginary part of the phaseshift must still be approximately determined (Miller 1970, Bieniek 1974, 1978). However, if it is large (e.g. the imaginary part of the complex phaseshift is not insignificant compared to unity), then the effects of the imaginary part of the potential on the initial wavefunction (and thereby on T-matrix elements) must be dealt with.

Although the imaginary width has been incorporated into quantum mechanical calculations (e.g., Hickman and Morgner 1976, Bieniek 1978, Waibel *et al* 1988, Padial *et al* 1989), we develop here a simple way of incorporating a complex potential into the evaluation of T-matrix elements by JWKB stationary-phase techniques. The final result needs little extra computational effort beyond the functions normally used, requiring only the additional calculation of a local imaginary phase for the entrance-channel JWKB wavefunction. In most situations, this can be done accurately with approximate expressions employing real quantities already computed. As will be shown below, the agreement with quantal complex-potential computations is excellent in the case of subthermal collisions of two $He^*(2^3S)$ metastables, and gives much insight into the causes of structure in both experimental (Müller *et al* 1987) and theoretical electron energy spectra.

2. Equations for cross sections

The full development of the formal equations for wavefunctions and cross sections can be found elsewhere (Bieniek 1978); the relevant ones are summarized here. The emitted PI/AI electrons can carry away angular momentum, producing a range of final-state heavy-particle angular momentum J'. However if only a few $\hbar$ are carried, the range of J' can often be adequately described in integrated energy spectra by their average value, which is just the entrance J (Bieniek 1978). Preliminary quantal calculations with and without his approximation (Müller *et al* 1990) did show some broadening due to rotational energy transfer, although not a large amount. Similar results were seen by Merz *et al* (1989, 1990) in $He^* + Li(Na)$ PI/AI systems, although there was a more noticeable effect in angular distributions. Since we are only concerned here with energy spectra integrated over all angles, we will assume the ejected electron has no significant amount of angular momentum.

Let $t(R)$ be the effective electronic coupling amplitude, as a function of internuclear separation R, between initial and final electronic potentials, incorporating the effects of all partial waves of the ejected electrons. The complex potential in the entrance channel is then $V_T(R) = V_i(R) - i\frac{1}{2}\Gamma(R)$, with the imaginary width $\Gamma(R) = 2\pi|t(R)|^2$. The Schrödinger equation for the corresponding radial wavefunction $\bar{F}_i^J(R)$ is

$$\left[-\frac{\hbar^2}{2m}\frac{d^2}{dR^2} + V_T(R) + \left(\frac{\hbar^2}{2m}\right)\frac{J(J+1)}{R^2} - E\right]\bar{F}_i^J(R) = 0 \tag{1}$$

where m is the collisional reduced mass, E and J the collisional energy and angular momentum. The bar over $\bar{F}_i^J$ indicates a complex quantity. $\bar{F}_i^J(R)$ has the asymptotic form

$$\begin{aligned}\bar{F}_i^J(R) &\sim k_i^{-1/2}\sin(k_iR - \tfrac{1}{2}J\pi + \delta_i^J + i\eta^J) \\ &\sim k_i^{-1/2}[\cosh(\eta^J)\sin(k_iR - \tfrac{1}{2}J\pi + \delta_i^J) + i\sinh(\eta^J)\cos(k_iR - \tfrac{1}{2}J\pi + \delta_i^J)]\end{aligned} \tag{2}$$

where δ_i^J and η^J are, respectively, the real and imaginary parts of the complex phase shift, and k_i is the asymptotic wavenumber. If $F_f^J(R)$ is the corresponding radial wavefunction for the final-state potential (which has no imaginary component), the differential cross section for the electron energy spectrum is:

$$\frac{d\sigma}{d\varepsilon} = \frac{4\pi^3}{k_i^2}\omega_i\sum_{J=0}^{J_{max}}(2J+1)|T_{if}^J(\varepsilon)|^2 \tag{3a}$$

where

$$T_{if}^{J}(\varepsilon) = \exp[\mathrm{i}(\delta_f^J + \delta_i^J)]T^J(\varepsilon) \tag{3b}$$

with

$$T^J(\varepsilon) = \frac{2m}{\hbar^2 \pi} \exp(-\eta^J) \int \bar{F}_i^J(R) t(R) F_f^J(R)\, \mathrm{d}R \tag{3c}$$

ω_i is the statistical weight of the heavy-particles in initial state i, and $J_{\max} = \infty$ (formally). $\mathrm{d}\sigma/\mathrm{d}\varepsilon$ can be written as

$$\frac{\mathrm{d}\sigma}{\mathrm{d}\varepsilon} = \frac{4\pi^3}{k_i^2} \omega_i \sum_{J=0}^{J_{\max}} (2J+1)|T^J(\varepsilon)|^2. \tag{4}$$

The main purpose of this paper is the evaluation of the effective T-matrix element $T^J(\varepsilon)$ by JWKB stationary-phase methods, and a discussion illustrating the interpretive usefulness of the consequent analytic forms.

The total cross section for PI and AI can be computed in two ways. One (σ_I) is simply to integrate the differential spectrum. Another (σ_O) is to employ the unitarity properties of the S-matrix to obtain a total cross section from the opacity function $O_J = 1 - \exp(-4\eta^J)$; i.e.

$$\sigma_\mathrm{I} = \int \frac{\mathrm{d}\sigma}{\mathrm{d}\varepsilon} \mathrm{d}\varepsilon \tag{5a}$$

$$\sigma_\mathrm{O} = \frac{\pi}{k_i^2} \omega_i \sum_{J=0}^{J_{\max}} (2J+1) O_J. \tag{5b}$$

σ_O is directly and formally based on the completeness of the set of final states, while one must compute these states individually to obtain σ_I. The degree of agreement between these two methods is a measure of the internal self-consistency of the wavefunctions employed to compute the differential spectra.

3. Stationary phase evaluation of $T(\varepsilon)$

3.1. Simple JWKB wavefunction in a complex potential

In the following presentation, we drop superscripts and subscripts that are obvious and not directly utilized in the discussion. Sufficiently far from the turning point, the simple JWKB wavefunction in the complex potential $V_T(R) = V_i(R) - \mathrm{i}\frac{1}{2}\Gamma(R)$ is given by (Chen 1967)

$$\bar{F}_i(R) = A_i(R) \sin[\Phi_i(R) + \mathrm{i}\mu(R)] \tag{6a}$$

where

$$A_i(R) = [K_i^J(R)]^{-1/2} \tag{6b}$$

$$\Phi_i(R) = \int_{R_\mathrm{t}}^{R} \mathrm{Re}[K_i^J(r)]\, \mathrm{d}r - D_\mathrm{t}^+ + \tfrac{1}{4}\pi \tag{6c}$$

$$\mu(R) = \int_{R_\mathrm{t}}^{R} \mathrm{Im}[K_i^J(r)]\, \mathrm{d}r + D_\mathrm{t}^-$$
$$= \frac{m}{2\hbar^2} \int_{R_\mathrm{t}}^{R} \frac{\Gamma(r)}{\mathrm{Re}[K_i^J(r)]} \mathrm{d}r + D_\mathrm{t}^- \tag{6d}$$

with

$$[K_i^J(R)]^2 = \frac{2m}{\hbar^2}[E_i - V_i^J(R) + \mathrm{i}\tfrac{1}{2}\Gamma(R)] \tag{6e}$$

$$V_i^J(R) = V_i(R) + \frac{\hbar^2}{2m}\frac{(J+\frac{1}{2})^2}{R^2} \tag{6f}$$

$$\mathrm{Re}[K_i^J(R)] = \left(\frac{2m}{\hbar^2}[\tfrac{1}{2}\{E - V_i^J(R)\} + \tfrac{1}{2}\{[E - V_i^J(R)]^2 + [\tfrac{1}{2}\Gamma(R)]^2\}^{1/2}]\right)^{1/2}. \tag{6g}$$

R_t is the turning point in the real potential, i.e. $V_i^J(R_t) = E_i$. $D_t^{\pm}$ are turning-point corrections given by

$$D_t^{\pm} = -\frac{1}{6}\left(\frac{2m}{\hbar^2}\right)^{1/2}[\Gamma(R_t)]^{3/2}\left[\frac{\dfrac{\mathrm{d}V_i^J}{\mathrm{d}R} \pm \dfrac{1}{2}\dfrac{\mathrm{d}\Gamma}{\mathrm{d}R}}{\left(\dfrac{\mathrm{d}V_i^J}{\mathrm{d}R}\right)^2 + \left(\dfrac{1}{2}\dfrac{\mathrm{d}\Gamma}{\mathrm{d}R}\right)^2}\right]_{R_t}. \tag{7}$$

Note that $D_t^{\pm} \to 0$ as $\Gamma(R_t) \to 0$. The wavefunction can be rewritten in a form that will prove more useful:

$$\bar{F}_i^J(R) = a_i(R)\,\mathrm{e}^{\mathrm{i}\vartheta(R)}\{\cosh[\mu(R)]\sin[\Phi_i(R)] + \mathrm{i}\sinh[\mu(R)]\sin[\Phi_i(R) + \tfrac{1}{2}\pi]\} \tag{8a}$$

where

$$a_i(R) = |A_i(R)| \tag{8b}$$

$$\vartheta(R) = \tan^{-1}\frac{\mathrm{Im}[A_i(R)]}{\mathrm{Re}[A_i(R)]}. \tag{8c}$$

For the simple JWKB wavefunction discussed so far

$$a_i(R) = |K_i^J(R)|^{-1/2} = \left(\frac{2m}{\hbar^2}\right)^{-1/4}\{[E - V_i^J(R)]^2 + [\tfrac{1}{2}\Gamma(R)]^2\}^{-1/8} \tag{9a}$$

$$\vartheta(R) = +\tfrac{1}{4}\tan^{-1}\frac{\Gamma(R)}{2[E - V_i^J(R)]}. \tag{9b}$$

The symbol $a(R)$ has been introduced because the amplitude will be modified later in situations near the turning point. For the evaluation of $T(\varepsilon)$, we also need the final-state wavefunction:

$$F_f(R) = a_f(R)\sin[\Phi_f(R)] \tag{10a}$$

where

$$a_f(R) = [k_f(R)]^{-1/2} \tag{10b}$$

$$\Phi_f(R) = \phi_f(R) + \tfrac{1}{4}\pi \tag{10c}$$

with

$$\phi_\alpha(R) = \int_{R_t}^{R} k_\alpha^J(r)\,\mathrm{d}r \tag{10d}$$

$$[k_\alpha^J(R)]^2 = \frac{2m}{\hbar^2}[E_\alpha - V_\alpha^J(R)] \tag{10e}$$

α is a channel index, and

$$V_\alpha^J(R) = V_\alpha(R) + \frac{\hbar^2}{2m}\frac{(J+\frac{1}{2})^2}{R^2}.$$

Note that the lower case k_α^2 is totally real, and will prove useful for both initial (i) and final (f) states.

3.2. *Location of stationary-phase points* R_s

We wish to find the stationary-phase points of the integrand of $T(\varepsilon)$ in (3c), from around which the major contributions to the integral occur. The integral for $T(\varepsilon)$ can be accurately written as

$$T(\varepsilon) = \frac{1}{2}\left\{\int e^{i\vartheta(R)} g(R)\cos[\Delta\Phi(R)]\,dR + i\int e^{i\vartheta(R)} h(R)\cos[\Delta\Phi(R) - \tfrac{1}{2}\pi]\,dR\right\} \quad (11a)$$

where

$$g^J(R) = \frac{2m}{\hbar^2\pi}\cosh[\mu^J(R)]\,e^{-\eta^J} a_i^J(R) a_f^J(R) t(R) \quad (11b)$$

$$h^J(R) = \frac{2m}{\hbar^2\pi}\sinh[\mu^J(R)]\,e^{-\eta^J} a_i^J(R) a_f^J(R) t(R)$$

$$= \frac{\sinh[\mu(R)]}{\cosh[\mu(R)]} g(R) \quad (11c)$$

with

$$\eta^J = \mu^J(\infty) \quad (11d)$$

$$\Delta\Phi(R) = \Phi_f(R) - \Phi_i(R). \quad (11e)$$

Rapidly oscillatory terms of the form $\cos[\Phi_i + \Phi_f]$ have been dropped from the integral of (11a).

A decision must now be made before the stationary-phase points can be found. The varying phase $\vartheta(R)$ [from $A_i(R)$] can be included with the phases found in the cosine factors of (11a) to produce general phase factors $\exp\{i[\Phi_f(R) - \Phi_i(R) \pm \vartheta(R)]\}$ in the integral, or it can be just associated with the prefactors $g(R)$ and $h(R)$. If it is included as a general phase, the number of stationary-phase points will be formally doubled. Since $\vartheta(R)$ is a slowly varying function in almost all situations, it is easier to treat it, along with $g(R)$ and $h(R)$, as a prefactor to the more rapidly changing cosine factors. With this in mind, the stationary phase points R_s of both integrals in (11a) are located where (Connor 1973, Child 1974)

$$\left.\frac{d\Delta\Phi}{dR}\right|_{R_s} = 0 \quad (12)$$

which is equivalent to

$$k_f^J(R_s) = \mathrm{Re}[K_i^J(R_s)]. \quad (13)$$

Letting $\Delta V(R) = V_i(R) - V_f(R)$, the R_s are related to the energy of the emitted electron ε by

$$\varepsilon = \Delta V(R_s) - Q(R_s) \tag{14a}$$

where

$$Q(R) = \tfrac{1}{2}[\{[E - V_i^J(R)]^2 + [\tfrac{1}{2}\Gamma(R)]^2\}^{1/2} - [E - V_i^J(R)]]. \tag{14b}$$

Defining a modified effective entrance-channel potential

$$U_i^J(R) = V_i^J(R) - Q(R) \tag{15}$$

the equations (14*a*) and (6*g*) can be rewritten as

$$\varepsilon = U_i^J(R_s) - V_f(R_s) \tag{16a}$$

$$\text{Re } K_i^J(R) = \left\{\frac{2m}{\hbar^2}[E - U_i^J(R)]\right\}^{1/2}. \tag{16b}$$

For R near a turning point $[(E - V_i^J(R)) \ll \Gamma(R)]$, $Q(R) \simeq \Gamma(R)/4$; for R far from a turning point $[(E - V_i^J(R)) \gg \Gamma(R)]$, $Q(R) \simeq \frac{1}{16}\Gamma^2(R)/(E - V_i^J)$. $Q(R)$ is usually very small (and actually negligible), and has little effect in most calculations. This was numerically confirmed in separate computations on the $He^*(2^3S) + He^*(2^3S)$ process considered in this paper.

Furthermore, it can be noted that in the limit $\Gamma(R) \to 0$, we find the usual conditions of

$$\varepsilon = \Delta V(R_s) \tag{17a}$$

and

$$k_f(R_s) = k_i(R_s). \tag{17b}$$

The stationary-phase points R_s are then just the J-independent Condon points R_c, where vertical transitions occur in a classical picture that conserves local heavy-particle linear momentum.

We will now consider explicitly two situations. The first is where there is only a single stationary-phase point, R_0, for a particular value of ε, giving rise to 'reflection' structures in the emission spectra; the second is where there are two points R_1 and R_2, producing rainbow interference structure (Tellinghuisen 1985).

Case 1. Single-stationary phase point. For a single, classically accessible solution $R_0(\varepsilon)$ of (14) (e.g. monotonic difference potentials), one can make a cubic fit to the phases at R_0, and evaluate $T(\varepsilon)$ analytically. Using an expression derived by Bieniek and Streeter (1983) for totally real potentials and by noting that the imaginary cosine integral in $T(\varepsilon)$ (equation (11*a*)) just differs from the real term by the phase $-\pi/2$, one finds for a single stationary-phase point that $T(\varepsilon)$ is given by (Bieniek and Streeter 1983)

$$T_0(\varepsilon) = Z(R_0, \xi_0, \rho_0) \tag{18a}$$

where

$$Z(R_s, \xi, \rho) = \rho^{1/4}(G_s^+ + iH_s^-)\,\text{Ai}(-\rho) + q_s\rho^{-1/4}(H_s^+ - iG_s^-)\,\text{Ai}'(-\rho) \tag{18b}$$

$$G_s^{\pm} = \tfrac{1}{2}(C_s + S_s)\cos(\xi + \vartheta_s) \pm \tfrac{1}{2}(C_s - S_s)\cos(\xi - \vartheta_s) \tag{18c}$$

$$H_s^{\pm} = \tfrac{1}{2}(C_s + S_s)\sin(\xi + \vartheta_s) \pm \tfrac{1}{2}(C_s - S_s)\sin(\xi - \vartheta_s) \tag{18d}$$

$$C_s = \frac{\pi g(R_s)}{|2\Delta\Phi''(R_s)|^{1/2}} = \frac{2m}{\hbar^2}\frac{\cosh(\mu_s^J)\exp(-\eta^J)a_i^J(R_s)a_f^J(R_s)t_s}{|2\Delta\Phi_s''|^{1/2}} \tag{18e}$$

$$S_s = \frac{\pi h(R_s)}{|2\Delta\Phi''(R_s)|^{1/2}} = \frac{2m}{\hbar^2}\frac{\sinh(\mu_s^J)\exp(-\eta^J)a_i^J(R_s)a_f^J(R_s)t_s}{|2\Delta\Phi_s''|^{1/2}} \tag{18f}$$

$$\xi_s = \Delta\Phi_s + \tfrac{2}{3}q_s(\rho_s)^{3/2} \tag{19a}$$

$$\rho_s = |\tfrac{1}{2}\Delta\Phi_s''|^2|\tfrac{1}{2}\Delta\phi_s'''|^{-4/3} \tag{19b}$$

$$q_s = \mathrm{sign}(\Delta\Phi_s''). \tag{19c}$$

A subscript of s indicates evaluation of the quantity at the stationary phase point R_s. $\mathrm{Ai}(x)$ is the regular, homogeneous Airy function.

The quantities C_s and S_s are, respectively, the coupling strengths that come from the real and imaginary parts of $\sqrt{K_i(R)}\bar{F}_i(R)$. (The C and S were chosen to remind one of the $\cosh\mu$ and $\sinh\mu$ factors in (8*a*).) These real and imaginary strengths appear together only because $K_i(R)$ is complex. If $\Gamma(R_s)$ is considered to be small compared to $E - V_i^J(R_s)$ everywhere, then it is reasonable to make the approximations

$$\vartheta(R) \simeq 0 \qquad \text{and} \qquad K_i(R) \simeq k_i(R). \tag{20}$$

(We will do this in all the numerical results reported below.) With these approximations,

$$G_s^+ = C_s\cos\xi \qquad H_s^+ = C_s\sin\xi$$
$$G_s^- = S_s\cos\xi \qquad H_s^- = S_s\sin\xi \tag{21}$$

$T_0(\varepsilon)$ then simplifies to

$$T_0(\varepsilon) = \rho_0^{1/4}\{[C_0\cos(\xi_0) + \mathrm{i}S_0\sin(\xi_0)]\,\mathrm{Ai}(-\rho_0) + q_0\rho^{-1/4}[C_0\sin(\xi_0) - \mathrm{i}S_0\cos(\xi_0)]\,\mathrm{Ai}'(-\rho_0)\} \tag{22}$$

The association of the coupling strength C_s (S_s) with the real (imaginary) part of the entrance channel wavefunction is now obvious through the $\cosh\mu_s(\sinh\mu_s)$ factors in C_s (S_s).

Case 2. Two interfering stationary-phase points. If $\Delta V(R)$ has an extremum, there will generally be two points of stationary phase, R_1 and R_2, that are solutions of (14). These two 'transition' points give rise to many interesting interference effects. If one again uses standard uniform methods (Connor 1973) to evaluate (11*a*), one obtains a T-matrix element $T_2(\varepsilon)$ for situations with two stationary-phase points:

$$T_2(\varepsilon) = [Z(R_1, u_{12}, y_{12}) + Z(R_2, u_{12}, y_{12})] \tag{23a}$$

where

$$u_{12} = \tfrac{1}{2}(\Delta\Phi_1 + \Delta\Phi_2) \tag{23b}$$

$$y_{12} = |\tfrac{3}{4}(\Delta\Phi_2 - \Delta\Phi_1)|^{2/3}. \tag{23c}$$

Note that the arguments of ξ_0 and ρ_0 in (18*a*) are replaced by u_{12} and y_{12}, which contain information from both points. u_{12} preserves information about the absolute phases relative to the turning points, while y_{12} produces inteference effects between R_1 and R_2. If we again make the approximation $\vartheta(R_s)=0$, we find

$$T_2(\varepsilon)=y_{12}^{1/4}[(C_1+C_2)\cos(u_{12})+\mathrm{i}(S_1+S_2)\sin(u_{12})]\,\mathrm{Ai}(-y_{12})$$
$$+q_1 y_{12}^{-1/4}[(C_1-C_2)\sin(u_{12})-\mathrm{i}(S_1-S_2)\cos(u_{12})]\,\mathrm{Ai}'(-y_{12}) \tag{24}$$

where we have used the fact $\mathrm{sign}(\Delta\Phi_1'')=-\mathrm{sign}(\Delta\Phi_2'')$. When R_1 and R_2 coalesce for ε at and beyond the extremum in $\Delta V(R)$, located at R_r where $\Delta V'(R_r)=0$, one can extend $T_2(\varepsilon)$ into the dark side of the classical rainbow singularity at $\varepsilon_r=\Delta V(R_r)$ in an accurate way described elsewhere (Sando and Wormhoudt 1973, Bieniek and Streeter 1983). Generally, the trigonometric functions $\cos(u_{12})$ and $\sin(u_{12})$ in (24) oscillate much more rapidly than the envelope demarcated by the Airy functions. This fact will prove the basis for much of the interpretive discussion of the numerical results for $\mathrm{He}^*(2^3\mathrm{S})+\mathrm{He}^*(2^3\mathrm{S})$ autoionization.

4. Turning points and barrier penetration

Before this can be done, a few finer points and nuances of an actual computation must be addressed. One is turning-point effects; another is penetration through a centrifugal barrier.

As a stationary-phase point R_s approaches a turning point R_t, the simple JWKB amplitudes $a_i^J(R_s)=a_f^J(R_s)=[k_i^J(R_s)]^{-1/2}\to\infty$, producing overly large coupling strengths C_s and S_s. A judicious choice of a convolution function may hide this problem, yet the accuracy must be suspected. Fortunately, the amplitudes can be prevented from becoming infinite by using modified amplitudes that are associated with uniform JWKB wavefunctions, which are valid near to and far from a turning point. These are given by (Bieniek 1980a)

$$a_{\alpha,\mathrm{u}}(R)=\pi^{1/2}\left[\frac{\chi_\alpha(R)}{k_\alpha^2(R)}\right]^{1/4}[\mathrm{Ai}^2(-\chi_\alpha)+\mathrm{Bi}^2(-\chi_\alpha)]^{1/2} \tag{25a}$$

where

$$\chi_\alpha(R)=[\tfrac{3}{2}\phi_\alpha(R)]^{2/3} \tag{25b}$$

for state α, with $\phi_\alpha(R)$ given by (10*d*). The phase $\Phi_\alpha(R)$ can be left unmodified. This produces a wavefunction which indeed has a large but infinite amplitude near R_t. Far from the turning point [i.e. $\phi_\alpha(R)\geqslant\pi$], $a_{\alpha,\mathrm{u}}(R)\simeq[k_\alpha(R)]^{-1/2}$. Thus the $a_{\alpha,\mathrm{u}}(R)$ can be directly substituted for $a_\alpha(R)$ in determining the coupling strengths of (18*e*,*f*). (Please note that this introduces no new functions into a computation and requires little additional computer time.)

With modified amplitudes, the coupling strengths C_s and S_s remain finite near a turning point. Unfortunately, both C_s and S_s then approach zero as $R_s\to R_t$ because $\Delta\Phi_s''\to\infty$ in (18*e*,*f*). Consequently, the contribution to a transition at a turning point is much smaller than usual, rather than larger. Yet this will generally produce little numerical error in a calculation of cross sections because R_t will be near a given $R_s(\varepsilon)$ for only a very few values of J, if any.

For situations with only a single stationary-phase point R_0, we can actually make a significant improvement over the use of modified amplitudes near a turning point.

We note that for R_0 near R_t, $\mu(R_0)$ is small [see (6*d*)]. This implies $\sinh \mu(R) \ll \cosh \mu(R)$ near R_0 in such cases, and $\bar{F}_i^J$ is almost totally real around R_0. Since most of the contribution to $T_0(\varepsilon)$ comes from around R_0, we have $\bar{F}_i^J \simeq \cosh \mu(R) a_{i,u}(R) \sin[\Phi_i(R)]$; i.e., the wavefunction acts as if it has arisen from the totally real potential $V_i^J(R)$, with a modified normalization of $\cosh \mu(R) \simeq 1$. We make the connection of this to the corresponding uniform JWKB wavefunction (Berry and Mount 1972):

$$\bar{F}_i^J(R) \simeq \cosh \mu(R) \pi^{1/2} \left[\frac{\chi_i(R)}{k_i^2(R)}\right]^{1/4} \mathrm{Ai}[-\chi_i(R)]. \tag{26}$$

Using the corresponding expression for the final-state wavefunction (without a cosh factor), one can analytically evaluate by stationary phase the overlap of these two uniform JWKB wavefunctions for a single R_0 (Bieniek 1977):

$$T_u(\varepsilon) = \frac{2m}{\hbar^2} e^{-\eta} \cosh(\mu_0) t_0 k_0^{-1} |2\Delta\phi_0''|^{-1/2} |\tfrac{3}{2}\Delta\phi_0|^{1/6} \mathrm{Ai}[p_0 |\tfrac{3}{2}\Delta\phi_0|^{2/3}] \tag{27}$$

where $p_0 = \mathrm{sign}(R_0 - R_t)$. This is valid even in the collisional inaccessible region of the repulsive inner core ($R_0 < R_t$).

$T_u(\varepsilon)$ will only be valid while $\sinh \mu(R_0) \ll \cosh \mu(R_0)$, i.e. near R_t. However, in most cases, by the time R_0 is sufficiently far from R_t so that this condition is no longer met, $\phi_{\min} = \min(\phi_i(R_0), \phi_f(R_0))$ is large enough ($\geq \pi$) that the simple JWKB wavefunction, equation (6*a*), is accurate; i.e. $T_u(\varepsilon)$ is accurate for $\phi_{\min} \leq \pi$ and $T_0(\varepsilon)$ is accurate when $\phi_{\min} \geq \pi$ (Bieniek 1980a). A smooth transition can be made between the two cases by defining a new T-matrix element $T_1(\varepsilon)$ for a single stationary-phase condition:

$$[\mathrm{Re}(T_1(\varepsilon))]^2 = w_0[\mathrm{Re}(T_0(\varepsilon))]^2 + (1 - w_0)[T_u(\varepsilon)]^2 \tag{28a}$$

$$[\mathrm{Im}(T_1(\varepsilon))]^2 = w_0[\mathrm{Im}(T_0(\varepsilon))]^2 \tag{28b}$$

where

$$w_0 = \min\left[1, \left(\frac{\phi_{\min}}{\phi_{us}}\right)^2\right] \tag{28c}$$

and ϕ_{us} is the chosen boundary between uniform and simple JWKB domains. ($\phi_{us} = \pi$ in this study, which produces wavefunctions accurate to within a few percent.)

The penetration of the JWKB wavefunction through the centrifugal barrier of the entrance channel must be included for accurate computations. $\bar{F}_i^J(R)$ will be reduced in the interior region by some factor $\exp(-\gamma_i^J)$. In the most simple approximation, $\gamma_i^J = 0$ if E_i is above the barrier peak. If E_i is lower than the barrier peak, located at R_{bp}^J, then

$$\gamma_i^J = \int_{R_{b1}}^{R_{b2}} |k_i^J(r)| \, dr$$

with R_{b1} and R_{b2} as the inner and outer turning points of the centrifugal barrier i.e. $E_i = V_i^J(R_{bn})$ (Child 1974). (More refined expressions for γ can be used to account for subtleties in the transmission and reflections coefficients, including undulations just above and below penetration (Bieniek 1974, Child 1976, Bieniek 1980a). Please note that the factor $-2/\pi$ in (14*a*) of Bieniek (1980a) should be $-\pi^{-1}$.) In all formula presented so far, each C_s and S_s must be multiplied by $e^{-\gamma_i^J}$ if $R_s < R_{bp}^J$. This decreases the coupling strengths. Furthermore, we must consider the effect of barrier penetration on the imaginary phase. One can show

$$\mu(R) \simeq \frac{m}{\hbar^2} \int_{R_t}^{R} [F_i^J(r)]^2 \Gamma(r) \, dr. \tag{29}$$

Replacing the $\sin^2$ in the integrand by its average of $\frac{1}{2}$, this expression simplifies to

$$\mu(R) \simeq \frac{m}{2\hbar} \int_{R_t}^{R} B(r) \frac{\Gamma(r)}{k_i^J(r)} \, dr + B(R_t) D_t^- \tag{30a}$$

where

$$B(r) = \begin{cases} e^{-2\gamma^J} & \text{if } R < R_{bp}^J \\ 1 & \text{if } R > R_{bp}^J \end{cases}. \tag{30b}$$

For low energy collisions, $\Gamma(R)$ is only large in the interior region ($R < R_{bp}^J$) once penetration occurs. In these cases, the correction represented by (30) is significant. If a computation of cross sections were cut off at J_{max} equal to the last J before barrier penetration, cross sections would be underestimated, for incident flux at higher J does indeed get into the interaction region. However, if $e^{-\gamma}$ were not introduced via C_s, S_s, and $B(R)$ into the computation, one would continue a computation to higher J with *no* natural cut-off. The calculation would not know that the imaginary potential should be 'felt' less in the interior region because of the smaller wavefunctional amplitudes. Cross sections (whether differential or total) would be overestimated. With these factors, cross sections will converge. In fact with the decrease of $\eta^J = \mu^J(\infty)$ following barrier penetration, one can simply use the opacity function as a convergence criterion; i.e. computations continue until a J_{max} value is reaches such that $O_{J_{max}}$ is less than some minimum value O_{min} chosen for a desired convergence.

5. Numerical treatment of the $He^*(2^3S) + He^*(2^3S)$ system

Two colliding metastable $He^*(2^3S)$ atoms follow a $^1\Sigma_g^+$, $^3\Sigma_u^+$ or $^5\Sigma_g^+$ potential. Because PI/AI is an electron transfer process, heavy-particle metastables that follow the $^5\Sigma_g^+$ potential do not participate in autoionization (Hill *et al* 1972). Therefore four transition amplitudes contribute to the process of the collision of two $He^*(2^3S)$ atoms:

$$He_2^*(^3\Sigma_u^+, J\text{-odd}) \rightarrow He_2^+(^2\Sigma_u^+, J'\text{-odd}) + e^-(l\text{-even}) \tag{31a}$$

$$He_2^*(^3\Sigma_u^+, J\text{-odd}) \rightarrow He_2^+(^2\Sigma_g^+, J'\text{-even}) + e^-(l\text{-odd}) \tag{31b}$$

$$He_2^*(^1\Sigma_g^+, J\text{-even}) \rightarrow He_2^+(^2\Sigma_u^+, J'\text{-odd}) + e^-(l\text{-odd}) \tag{31c}$$

$$He_2^*(^1\Sigma_g^+, J\text{-even}) \rightarrow He_2^+(^2\Sigma_g^+, J'\text{-even}) + e^-(l\text{-even}) \tag{31d}$$

where J (J') is the heavy particle angular momentum in the entrance (exit) channel, and l is the angular momentum of the ejected electron.

In our numerical treatment, we used transitions (31*a*) (attractive exit channel) and (31*d*) (repulsive exit channel) as model cases. We employed the entrance-channel potentials of Müller *et al* (1987) and the exit-channel potentials of Khan and Jordan (1986). Following Garrison *et al* (1973), we used the same effective imaginary width for the similar $^3\Sigma_u^+$ and $^1\Sigma_g^+$ entrance potentials, given by $\Gamma(R) = \Gamma_0 \exp(-aR)$, with $\Gamma_0 = 8.163$ eV and $a = 0.921\ a_0^{-1}$. In all calculations, we neglect the nuclear symmetry effects (indicated by the angular momenta in (31)) in this homonuclear collision. (Additional calculations including those by Müller *et al* (1990) showed no noticeable consequence.) Furthermore, final bound and quasibound levels in the stationary-phase calculations were smeared into a continuum, and were represented with wavefunctions in the form of (10). This essentially releases the boundary condition at the right-hand turning point. This is a good approximation if energy spectra are convoluted by an

instrument function whose width is too large to resolve rovibronic level spacing. Finally, all stationary phase calculations assumed $\mathrm{Re}[K_i^J(R)] = k_i^J(R)$ and $\vartheta(R_s) = 0$. Consequently, the R_s are equal to the J-independent Condon points of (17*a*).

The electron energy spectra for $^1\Sigma_g^+ \rightarrow {}^2\Sigma_g^+$ and $^3\Sigma_u^+ \rightarrow {}^2\Sigma_u^+$ transitions, at a collisional energy of $E_i = 1$ meV (chosen to match the experiment of Müller *et al* (1987)) are shown in figure 1. The electron energy scales have been shifted by the asymptotic transition energy $\varepsilon_0 = \Delta V(\infty)$. The JWKB stationary-phase curves are based on all the techniques and modifications presented above. The computational cut-off criterion was chosen to be $O_{\min} = 0.01$, which made $J_{\max} = 15$, the first J with centrifugal-barrier penetration. Also displayed in this figure are the spectra obtained with a quantum mechanical complex-potential computer code, in which all wavefunctions and matrix elements were calculated wholly numerically. In order to simulate the experimental results (Müller *et al* 1987) more closely, all spectra were convoluted by a Gaussian function of width 36 meV. This explains the lack of discrete structure for the AI portion of the $He_2^*(^3\Sigma_u^+) \rightarrow He_2^+(^2\Sigma_u^+)$ spectrum (figure 1(*a*)).

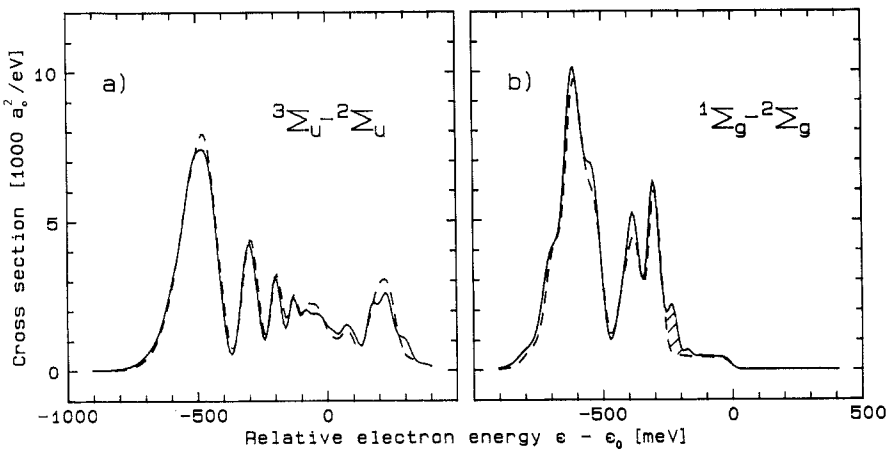

Figure 1. Comparison of uniform complex, stationary-phase calculations with quantum mechanically calculated electron energy spectra for the transitions $^3\Sigma_u^+ \rightarrow {}^2\Sigma_u$ and $^1\Sigma_g \rightarrow {}^2\Sigma_g$ at a collisional energy of $E_i = 1$ meV. The spectra are convoluted by 36 meV (FWHM) gaussian, and shifted by $\varepsilon_0 = \Delta V(\infty) = 15.052$ eV. The hatched region is due to the tunnelling into the repulsive wall (see text).

Note that the stationary-phase and quantal results are compared on an absolute scale. The agreement is most satisfying. The total JWKB cross sections obtained from opacity functions were $\sigma_O(^1\Sigma_g^+ \rightarrow {}^2\Sigma_g^+) = 2661\ a_0^2$ and $\sigma_O(^3\Sigma_u^+ \rightarrow {}^2\Sigma_u^+) = 2659\ a_0^2$. These differed by less than 1% from the quantal values. This illustrates the importance of barrier penentration. If the JWKB computations were terminated just before the onset of penetration of the centrifugal barrier (i.e., setting $J_{\max}$ equal to 14) then the cross sections were 13% too low. If $J_{\max} = 15$ were chosen but (6*d*), instead of (30*a*), was used to determine $\eta^{J_{\max}} = \mu^{J_{\max}}(\infty)$, then the JWKB total cross sections were about 15% too high.

However, the JWKB total cross sections σ_O obtained from opacity functions are not a stringent test of the stationary-phase technique. JWKB σ_O will generally be in good agreement with quantal results as long as O_J is nearly unity before the onset of centrifugal-barrier penetration, and falls off rapidly over a small range of J following

penetration. This is the case for homonuclear He*(2^3S) collisions. A much more stringent test is the JWKB integrated cross section σ_I (equation (5*a*)). It is most gratifying that $\sigma_I(^3\Sigma_u^+ \rightarrow {}^2\Sigma_u^+) = 2689\ a_0^2$, making $\sigma_I/\sigma_O = 1.01$ and also within 1% of the quantal value. This indicates that the delicate balance of amplitudes and phases, and their localized contributions around R_s, are accurately represented by the presented formulae, both the real and imaginary parts. For $^1\Sigma_g^+ \rightarrow {}^2\Sigma_g^+$ transitions, the JWKB $\sigma_I(^1\Sigma_g^+ \rightarrow {}^2\Sigma_g^+) = 2389\ a_0^2$, giving $\sigma_I/\sigma_O = 0.90$. This discrepancy is mostly due to the underestimation of $d\sigma/d\varepsilon$ for electron energies $\varepsilon - \varepsilon_0 \approx -275$ meV (see figure 1(*b*)). Both electron spectra in figure 1 exhibit well the rainbow phenomena (Airy-terms in equation (24)) caused by the extremum in the difference potential.

Through stationary-phase analysis, one can readily perceive the relationship between potentials and structure in the spectra. In figure 2, we show this relationship for the $^1\Sigma_g^+ \rightarrow {}^2\Sigma_g^+$ transition. To emphasize the import of the turning points, we have employed simple JWKB amplitudes $a_\alpha^J(R_s) = [k_\alpha^J(R_s)]^{-1/2}$ throughout the calculation of this spectrum and have not convoluted it. The R_s are located where $\Delta\varepsilon = \varepsilon - \varepsilon_0$ crosses the potential difference curve. For $\Delta\varepsilon > 0$, there is only one stationary-phase point, R_0. For $\Delta\varepsilon < 0$ there are two, R_1 and R_2. However, the turning point R_t^* in the entrance (metastable) channel is located at a position ($\simeq 4.4\ a_0$ over the relevant J-range) such that two points are collisionally accessible only for $\Delta\varepsilon < -250$ meV. The Airy-peak in the spectrum, at $\Delta\varepsilon \simeq -600$ meV, is due to the extremum in $\Delta V(R)$. As $\Delta\varepsilon$ increases from -600 meV to -250 meV, the inner stationary-phase point R_1 approaches R_t^*. $a_\alpha(R_1)$ is getting larger, producing larger coupling strengths C_1 and S_1 in equation (24). This is why $d\sigma/d\varepsilon$ increases so dramatically between -300 meV to -250 meV. (The only reason it does not go to infinity at some point is that none of the $R_1(\varepsilon)$ associated with the chosen electron-energy grid points happen to land directly on R_t^* for any J.) For $\Delta\varepsilon > -250$ meV, only the outer point R_2 is collisionally accessible. Since this is associated with a low $t(R)$ because of the large separation, $d\sigma/dE$ falls off percipitously as the T-matrix element switches from $T_2(\varepsilon)$ to $T_1(\varepsilon)$. (It is unfortunate

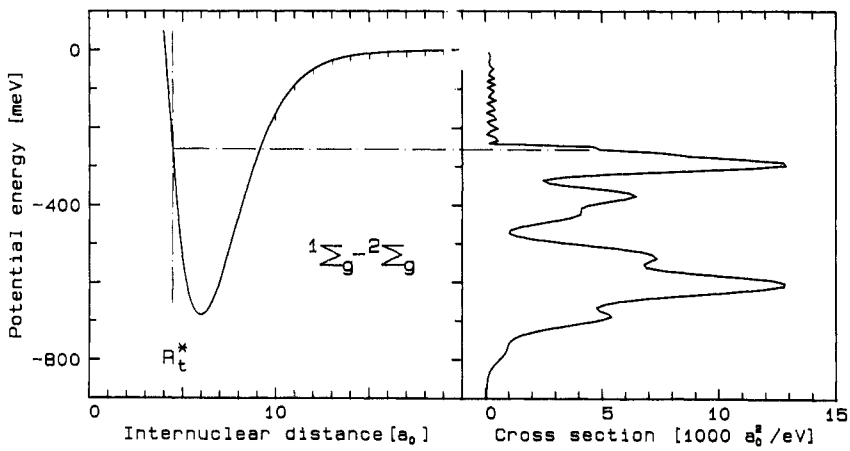

Figure 2. Correlation of the difference potential energy (left half) and the electron spectrum (right half) for transition $^1\Sigma_g \rightarrow {}^2\Sigma_g$. Condon points R_c to the left of R_t^* (the turning point in the entrance channel for 1 meV collisions) are not classically accessible, while those to the right of it are. Thus for $\varepsilon - \varepsilon_0 \geqslant -250$ meV, only one point of stationary phase in the marked long-range part of the difference potential contributes to the electron spectrum, which was calculated using only simple JWKB wavefunctional amplitudes.

that no uniform formula exists (Uzer and Child 1982) for $T_2(\varepsilon)$ for two stationary-phase points, one of which is in a classically inaccessible region, for this would eliminate the small discrepancy between JWKB and quantal $d\sigma/d\varepsilon$ around $\Delta\varepsilon \approx -275$ meV in figure 1(*b*).) By comparing the $^1\Sigma_g^+ \rightarrow {}^2\Sigma_g^+$ in figures 1(*b*) and 2, one can see the importance of using uniform JWKB amplitudes (equation (25)) instead of just simple JWKB amplitudes, for the latter significantly overestimates the increase in peak height due to turning-point effects.

Similar arguments can be used for the $^3\Sigma_u^+ \rightarrow {}^2\Sigma_u^+$ spectrum. The difference potential is similar in shape and magnitude to the $^1\Sigma_g^+ \rightarrow {}^2\Sigma_g^+$ curve, but is shifted to larger internuclear separations by about $0.5\,a_0$. This makes both R_1 and R_2 collisionally accessible for $\Delta\varepsilon < 0$ (PI), and a single R_0 accessible for $\Delta\varepsilon > 0$ (AI). $\Delta\varepsilon = 0$ is effectively the boundary between PI and AI because $E_i = 1$ meV is so small on the scale of $\Delta V(R)$ in the interaction region.

To understand the sources of structure and the conditions that moderate them, it is useful to consider only the dominate terms in $|T_2(\varepsilon)|$. The $\mathrm{Ai}'(-y_{12})$ term in (24) is small compared to the $\mathrm{Ai}(-y_{12})$ term in this system, as is usually the case in rainbow spectra. If we neglect this term and cross terms, we find the differential cross section to be

$$\frac{d\sigma}{d\varepsilon} \simeq \frac{4\pi^3}{k_i^2}\,\omega_i \sum_{J=0}^{J_{max}} (2J+1)|T_2^J(\varepsilon)|^2_{dom} \tag{32a}$$

where

$$|T_2^J(\varepsilon)|^2_{dom} = y_{12}^{1/4}[(C_1+C_2)^2\cos^2(u_{12}^J) + (S_1+S_2)^2\sin^2(u_{12}^J)]\,\mathrm{Ai}^2(-y_{12}) \tag{32b}$$

where the $(C_1+C_2)^2$ term arises from the real parts of the entrance-channel wavefunction $\bar{F}_i^J(R)$ of (8*a*) and of $T_2(\varepsilon)$ of (24), and the $(S_1+S_2)^2$ term comes from the imaginary parts. The superscript J is explicitly shown on the most J-sensitive element.

Let us now consider the contribution from the 'real' portion of (32*b*), and examine the effect of phase-averaging due to the sum over angular momenta. Figure 3 displays

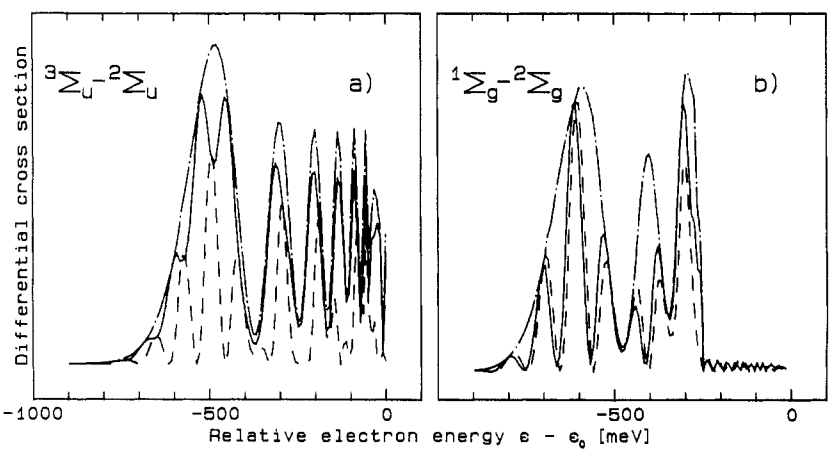

Figure 3. J-dependence of the electron spectra for the transition $^3\Sigma_u \rightarrow {}^2\Sigma_u$ (figure 3(*a*)) and $^1\Sigma_g \rightarrow {}^2\Sigma_g$ (figure 3(*b*)). The broken curves are spectra for $J = 0$, multiplied by a factor of 100 (figure 3(*a*)) and 200 (figure 3(*b*)). The full curves represent the spectrum summed over $J = 0$–15 partial waves ($E_i = 1$ meV). Additionally, the Ai^2-envelope, produced by replacing $\cos^2(u)$ in equation (24) with $\frac{1}{2}$, are indicated by the chain curves.

the spectra obtained by ignoring the imaginary contribution to (32*b*), and plots the computed spectra for $J_{max}=0$ (i.e. $J=0$ only), $J_{max}=15$, and $J_{max}=15$ with $\cos^2(u)$ replaced by 1/2. (As in figure 2, simple JWKB amplitudes are used, and the spectra are not convoluted.) The latter approximation shows the Airy-envelope. One can see in both transitions the rapid oscillations typical for a single J due to the $\cos^2(u_{12})$ factor; this is reminiscent of the spectra from bound-free spectral processes discussed in the introduction. However, once the sum over J is made, the rapid oscillations have been largely washed out for the $^3\Sigma_u^+ \rightarrow {}^2\Sigma_u^+$ transition, but not for the $^1\Sigma_g^+ \rightarrow {}^2\Sigma_g^+$ transition. The former nearly achieves the pure slow undulations of the Airy envelope because of the larger degree of phase-averaging of u_{12}^J over J; i.e. $\langle \cos^2 u_{12}^J(\varepsilon)\rangle^2$ is actually about $\frac{1}{2}$ for all ε. More phase-averaging occurs in the $^3\Sigma_u^+ \rightarrow {}^2\Sigma_u^+$ because of differences in turning points $\Delta R_t = |R_t^*(E_i) - R_t^+(\varepsilon)|$ between metastable and ionic channels for ε in the region of the Airy maximum. ΔR_t is larger ($\simeq 2.5\ a_0$) for the $^3\Sigma^+ \rightarrow {}^2\Sigma_u^+$ transition than for the $^1\Sigma_g^+ \rightarrow {}^2\Sigma_g^+$ case ($\simeq 1.0\ a_0$). Thus as J increases in the first transition, there is a larger distance between turning points and stationary-phase points over which the phase between initial and final wavefunctions can be affected by J than for the $^1\Sigma_g^+ \rightarrow {}^2\Sigma_g^+$ transition. This generates a more rapidly changing u_{12}^J with J, and a more random $\cos^2(u_{12}^J)$. By shifting the $He_2^+(^2\Sigma_g^+)$ potential to smaller internuclear distances, thereby increases $\Delta R_t(^1\Sigma_g^+ \rightarrow {}^2\Sigma_g^+))$ to match $\Delta R_t(^3\Sigma_u^+ \rightarrow {}^2\Sigma_u^+)$, we were able to generate the strong phase-averaging found in the $^3\Sigma_u^+ \rightarrow {}^2\Sigma_u^+$ transition, confirming our analysis (Müller *et al* 1990).

Figure 4 displays the real contributions to $d\sigma/d\varepsilon$ in comparison to the full differential cross sections; all spectra have been convoluted and uniform amplitudes $a_{\alpha,u}(R_s)$ employed. The difference between each pair of spectra comes from the imaginary parts of $\bar{F}_i^J$ and of $T_2^J(\varepsilon)$, i.e. the $(S_1+S_2)^2\sin^2(u)$ term in (32). As can be seen, the imaginary contribution is significant. Furthermore, it fills in almost all rapid-oscillation effects. Even in the $^1\Sigma_g^+ \rightarrow {}^2\Sigma_g^+$ transition, only some shoulders on both sides of the Airy peak are noticeable. The cause of this is universal and enlightening. Consider two limiting case: $\mu(R_s)$ small compared to unity, and $\mu(R_s)$ large. These are essentially low-Γ (weak coupling) and high-Γ (strong coupling) cases. For small $\mu(R_s)$, $\sinh\mu_s \ll \cosh\mu_s$, yielding $(S_1+S_2) \ll (C_1+C_2)^2$ (see equations (18*e*) and (18*f*)). In contrast, if $\mu(R_s)$ is large, $\sinh\mu_s \simeq \cosh\mu_s$, implying $(S_1+S_2)^2 \simeq (C_1+C_2)^2$. We then have

$$|T^J(\varepsilon)|^2_{dom} = \begin{cases} y_{12}^{1/4}(C_1+C_2)^2\cos^2(u_{12}^J)\,\mathrm{Ai}^2(-y_{12}) & \text{for small } \mu_s \\ y_{12}^{1/4}(C_1+C_2)^2\,\mathrm{Ai}^2(-y_{12}) & \text{for large } \mu_s. \end{cases} \tag{33}$$

For low Γ, the rapid-oscillation factor $\cos^2(u_{12}^J)$ is preserved, allowing hope that these oscillations can be observed in subthermal collisions with little phase-averaging. However, for high Γ, no rapid oscillations can occur. As has almost completely happened in the $^1\Sigma_g^+ \rightarrow {}^2\Sigma_g^+$ case, high Γ tends to destroy rapid oscillations. This can be understood by thinking of the rapid oscillations as arising from interference between incoming and outgoing waves. Their relationship is contained in the absolute phase functions in (32). As Γ gets larger and more flux is lost to transitions, there is less and less outgoing wave with which to interfer with the incoming wave. Thus the rapid oscillations are filled in.

We find, then, that the contribution of the imaginary part of the entrance-channel wavefunction is significant, even when $\Gamma(R)$ is not really large compared to the real-part of the potential. The condition is if $\tanh[\mu(R_s)]$ is significant compared to unity. To clearly demonstrate the importance of the imaginary terms, we show in figure 5 the spectra for two extrema in magnitude of the autoionization width. The spectra compared

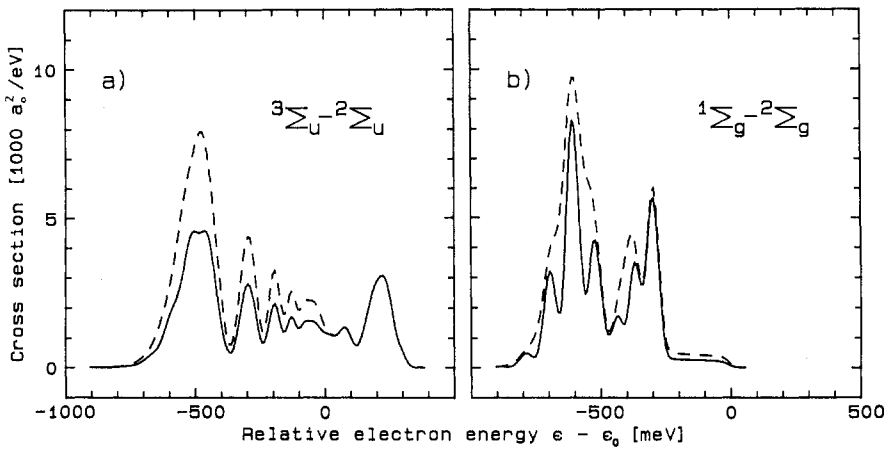

Figure 4. Comparison of uniform complex stationary-phase calculations (broken curve) with the corresponding spectra obtained from only the real part (full curve) of T-matrix elements. All spectra are convoluted with 36 meV (FWHM).

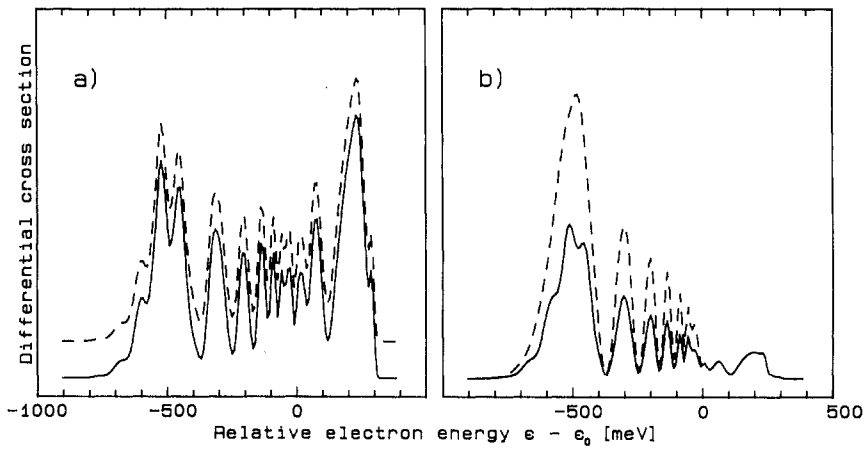

Figure 5. Comparison of stationary phase calculations using the real part of $T(\varepsilon)$ (full curve) and the full complex $T(\varepsilon)$ (broken curve) for transition $^3\Sigma_u \rightarrow {}^2\Sigma_u$ and two different widths Γ_1 (figure 5(a)) and Γ_2 (figure 5(b)) defined in the text. The base line is shifted for the two spectra, in figure 5(a), because they are essentially identical.

in this figure are calculated using; (1) only the real part of $T(\varepsilon)$ (full curve), and (2) a complete complex description (broken curve). The widths are as follows:

$$\text{Figure } 5(a) \quad \Gamma_1 = 0.8163 \text{ meV} \exp(-0.921\ R/a_0) = 10^{-4}\Gamma_0(R) \tag{34a}$$

$$\text{Figure } 5(b) \quad \Gamma_2 = 16.326 \text{ eV} \exp(-0.921\ R/a_0) = 2\Gamma_0(R) \tag{34b}$$

where $\Gamma_0(R)$ is the width used in the computations already discussed in figures 1-4. This leads to typical opacities of $O(\Gamma_1) = 5 \times 10^{-4}$ and $O(\Gamma_2) = 1.00$. Because the potential with Γ_1 is approximately real, the real and complex description of $d\sigma/d\varepsilon$ are identical (figure 5(a)). For Γ_2, the autoionization probability is 100% on the incoming trajectory, and the loss of flux cannot be neglected. As can be seen in figure 5(b), the oscillations due to incoming-outgoing interferences are no longer visible in

a full complex calculation at high Γ, while a real calculation still erroreously shows these oscillations. The fact that shoulders are indeed observed in the experimental spectrum of Müller *et al* (1987) implies that the actual $\Gamma(R)$ is not as large as $\Gamma_2(R)$.

6. Conclusion

For collisional systems with strong transitional coupling, the perturbation on the entrance channel from transitions can be conveniently described by a complex (optical) potential. We have shown how JWKB stationary-phase methods of analytically evaluating T-matrix elements, which have worked so well in the analysis of real-potential processes such as photon emission and absorption, can be easily extended to complex potential processes. In the case of Penning and associative ionization in the $He^*(2^3S) + He^*(2^3S)$ system, where autoionization is nearly 100%, the stationary-phase results were brought into impressive numerical agreement with quantum mechanical calculations, through use of an approximate complex phase, simple JWKB centrifugal-barrier penetration factors, and uniform JWKB amplitudes. The imaginary part of the entrance-channel wavefunction had a large effect on the energy spectra of the ejected electrons. The analytic form of the stationary-phase expressions associated with the complex potential give much insight and clarity to the analysis of the sources of structure in the spectra, particularly rapid and slow oscillations. It was shown how angular-momenta phase averaging and a large imaginary width both tend to wash out rapid oscillations. However, in subthermal collisions, the effect of rapid oscillations may still be discerned as shoulders in the primary rainbow peaks of spectra, for moderate imaginary widths.

Acknowledgment

The authors wish to thank the Deutsche Forschungsgemeinschaft (SFB 91) for their support, and acknowledge in particular the congenial and beneficial hospitality of Professor H Hotop and his group. We are grateful to Professor W Meyer for supplying the quantum mechanical complex-potential computer code utilized in this project. R J Bieniek would also like to thank the Fulbright Kommission of the Bundesrepublik Deutschland for a Senior Professorship during this work.

References

Bell K L 1970 *J. Phys. B: At. Mol. Phys.* **3** 1308
Berman M, Cederbaum L S and Domcke W 1983 *J. Phys. B: At. Mol. Phys.* **16** 875
Berry M V and Mount K E 1972 *Rep. Prog. Phys.* **35** 315
Bieniek R J 1974 *J. Phys. B: At. Mol. Phys.* **7** L266
—— 1977 *Phys. Rev.* A **15** 1513
—— 1978 *Phys. Rev.* A **18** 392
—— 1980 *J. Chem. Phys.* **72** 1225; (E) **73** 4712
—— 1980 *J. Phys. B: At. Mol. Phys.* **13** 4405; (C) **14** 1707
Bieniek R J and Streeter T J 1983 *Phys. Rev.* A **28** 3328
Cermak V and Herman Z 1968 *J. Chem. Phys. Lett.* **2** 359
Chen J C Y 1967 *Phys. Rev.* **156** 12
Child M S 1974 *Molecular Collision Theory* (London: Academic Press)
—— 1976 *Mol. Phys.* **31** 1031

Connor J N L 1973 *Mol. Phys.* **25** 181
Eisel D, Zevgolis D and Demtröder W 1979 *J. Chem. Phys.* **71** 2005
Fano U 1961 *Phys. Rev.* **124** 1866
Gadea F X, Spiegelmann F, Castex M C and Morlais M 1983 *J. Chem. Phys.* **78** 7270
Garrison B J, Miller W H and Schaefer H F 1973 *J. Chem. Phys.* **59** 3193
Gerber G and Niehaus A 1976 *J. Phys. B: At. Mol. Phys.* **9** 123
Hickman A P and Morgner H 1976 *J. Phys. B: At. Mol. Phys.* **9** 1765
Hill J C, Hatfield L L, Stockwell N D and Walters G K 1972 *Phys. Rev.* A **5** 189
Hotop H and Niehaus A 1968 *Z. Phys.* **215** 395
—— 1969 *Z. Phys.* **228** 68
—— 1970 *Z. Phys.* **238** 452
—— 1970 *Z. Phys.* D **238** 452
Jones D M and Dahler J S 1988 *Phys. Rev.* A **37** 2916
Khan A and Jordan K D 1986 *Chem. Phys. Lett.* **128** 368
Lam K-S and George T F 1984 *Phys. Rev.* A **29** 492
Master M, Huennekens J, Luh W-T, Li L, Lyrra A M, Sando K, Zafiropulos V and Stwalley W C 1990 *J. Chem. Phys.* **92** 5801
Merz A, Müller M W, Ruf M-W, Hotop H, Meyer W and Movre M 1989 *Chem. Phys. Lett.* **160** 337
—— 1990 *Chem. Phys.* **145** 219
Miller W H 1970 *J. Chem. Phys.* **52** 3563
Morgner H 1990 *Chem. Phys.* in press
Morgner H and Niehaus A 1979 *J. Phys. B: At. Mol. Phys.* **12** 1805
Mori M 1969 *J. Phys. Soc. Japan* **26** 773
Müller M W, Bußert W, Ruf M-W, Hotop H and Meyer W 1987 *Phys. Rev. Lett.* **59** 2279
Müller M W, Ruf M-W, Hotop H, Movre M and Meyer W to be published in *Z. Phys.* D
Mündel C and Domcke W 1984 *J. Phys. B: At. Mol. Phys.* **17** 3593
Nakamura H 1968 *J. Phys. Soc. Japan* **24** 1353
—— 1968 *J. Phys. Soc. Japan* **25** 519
—— 1969 *J. Phys. Soc. Japan* **26** 614
Niehaus A 1990 *Phys. Rep.* **186** 149
Noll T and Schmoranzer H 1987 *Phys. Scr.* **36** 129
O'Malley T F 1967 *Phys. Rev.* A **156** 230
Padial N T, Cohen J S, Martin R L and Lane N F 1989 *Phys. Rev.* A **40** 117
Saha H P, Dahler J S and Nielsen S E 1983 *Phys. Rev.* A **28** 1487
Sando K M and Wormhoudt J C 1973 *Phys. Rev.* A **7** 1889
Sayer B, Ferray M, Visticot J P and Lozingto J 1980 *J. Phys. B: At. Mol. Phys.* **13** 177
Schmeltekopf A L and Gilman G I 1967 *Planet. Space Sci.* **15** 401
Schmoranzer H, Noll T, Roueff E, Abgrall H and Bieniek R J 1990 *Phys. Rev.* A **42** 1835
Szudy J and Baylis W E 1975 *J. Quant. Spectrosc. Radiat. Transfer* **15** 641
Tellinghuisen J 1985 *Adv. Chem. Phys.* **60** 299
Tellinghuisen J, Pichler G, Snow W L, Hillard M E and Exton R J 1980 *Chem. Phys.* **50** 313
Uzer T and Child M S 1982 *Mol. Phys.* **46** 1371
Waibel H, Ruf M-W and Hotop H 1988 *Z. Phys.* D **5** 9
Weiner J, Masnou-Seeuws F and Giusti-Suzor A 1990 *Adv. At. Mol. Opt. Phys.* **26** 209